

Ab initio calculations of low-lying electronic states of vinyl chloride

Jia-Lin Chang

Institute of Atomic and Molecular Sciences, Academia Sinica, P.O. Box 23-166, Taipei 106, Taiwan, Republic of China and Department of Science Education, National Taichung Teachers College, Taichung 403, Taiwan, Republic of China

Yit-Tsong Chen^{a)}

Institute of Atomic and Molecular Sciences, Academia Sinica, P.O. Box 23-166, Taipei 106, Taiwan, Republic of China, and Department of Chemistry, National Taiwan University, Taipei 106, Taiwan, Republic of China

(Received 27 November 2001; accepted 8 February 2002)

The equilibrium geometries, vibrational frequencies, excitation energies, and oscillator strengths of vinyl chloride in the ground and five lowest-lying excited singlet states have been calculated using MP2, CIS, CASSCF, and MRCI methods with the 6-311++G** basis set. The geometries and vibrational frequencies of the ground and excited states are utilized to compute Franck–Condon factors. Calculated vibronic spectra for the transitions from the ground state to these five excited states are in agreement with experiment at 52 500–60 000 cm⁻¹, with major contributions from the $\tilde{A}(1^1A'') \leftarrow \tilde{X}(1^1A')$ and $\tilde{C}(2^1A') \leftarrow \tilde{X}(1^1A')$ transitions. In this study, two spin-forbidden transitions of $\tilde{b}(1^3A'') \leftarrow \tilde{X}(1^1A')$ and $\tilde{c}(2^3A'') \leftarrow \tilde{X}(1^1A')$ are calculated to locate in 45 000–54 000 cm⁻¹, and could be responsible for the observed one-photon absorption spectrum due to an intensity borrowing caused by the spin–orbit coupling of the Cl atom. Based on calculation, we speculate that upon the excitation of vinyl chloride at 193 nm the $\tilde{b}(1^3A'')$ or $\tilde{c}(2^3A'')$ excited state, instead of the (π, π^*) , is initially prepared prior to the subsequent photodissociation processes.

© 2002 American Institute of Physics. [DOI: 10.1063/1.1466828]

I. INTRODUCTION

Despite being an atmospheric pollutant, vinyl chloride (VC, C₂H₃Cl) has been widely used in the industry for poly(vinyl chloride) production. The understanding of its photochemistry and spectroscopy is therefore very important. The photodissociation dynamics of VC has been studied extensively by many researchers, for example, Gordon and co-workers,^{1–5} Blank *et al.*,⁶ Tonokura *et al.*,⁷ Donaldson and Leone,⁸ Moss *et al.*,⁹ Lee and co-workers,¹⁰ and Umemoto *et al.*¹¹ Walsh,¹² Sood and Watanabe,¹³ Berry,¹⁴ and Lochter *et al.*¹⁵ investigated the one-photon absorption spectra of VC below the first ionization energy. In addition, Koerting *et al.*¹⁶ observed a triplet–singlet transition of VC using electron impact ionization spectroscopy. Moreover, both infrared and microwave spectra of VC have been explored in great detail.^{17–27} Robin²⁸ reviewed the early studies before 1984 on the excited electronic states of chloroethylenes.

Recently, we have analyzed the 2+1 resonance-enhanced multiphoton ionization (REMPI) spectra of VC in the energy region of 7.3–10 eV, from which the adiabatic ionization energy (AIE) of VC is determined to be 80 720 ± 6 cm⁻¹ (10.0080 ± 0.0007 eV),^{29,30} in agreement with that obtained by photoelectron spectroscopy.^{31–36} Our work, in conjunction with a previous REMPI study on VC by Williams and Cool,³⁷ provide valuable insights into the excited states involved in the photodissociation dynamics of VC at 7.3–10

eV. Below 7.3 eV, the absorption spectrum of VC reported by Berry¹⁴ shows a broad and continuous band, yet with some weak features. The observed spectrum, however, has so far been only partially assigned, and little is known about the true identities of the excited states.

In the theoretical studies of VC, Umemoto *et al.*¹¹ calculated the relative energies for the four excited states of (π, σ_{C-Cl}^*) , (π, π^*) , (n_{Cl}, π^*) , and $(n_{Cl}, \sigma_{C-Cl}^*)$. The vertical excitation energies of these four states were later calculated by Tonokura *et al.*⁷ using complete active space self-consistent field (CASSCF) and internally contracted multi-reference configuration interaction (MRCI) methods. Browning *et al.*³⁸ applied a configuration interaction (CI) method with single excitation (CIS) to calculate the C–Cl antibonding character in the (π, π^*) excited state of VC. Utilizing restricted Hartree–Fock and CI with single and double excitation approaches, Takeshita³⁹ calculated the AIE and Franck–Condon factors (FCF) for the transitions to the ionic state of VC. On the other hand, Riehl and Morokuma⁴⁰ studied the unimolecular dissociation of VC on the ground-state potential energy surface using second-order Møller–Plesset (MP2) and quadratic single and double CI including a triple contribution. Colegrove and Thompson⁴¹ determined the heats of formation of VC and other chlorinated hydrocarbons with *ab initio* calculations. To date, however, neither adiabatic excitation energies nor molecular Rydberg states of VC have been calculated by theoretical methods.

In this work, we have performed *ab initio* calculations of both vertical and adiabatic excitation energies, oscillator strengths, and FCFs for the five lowest-lying excited singlet

^{a)} Author to whom correspondence should be addressed. Electronic mail: ytchen@pub.iam.s.sinica.edu.tw

states of VC, i.e., $(\pi, 3s/\sigma_{C-Cl}^*)$, $(\pi, \sigma_{C-Cl}^*/3s)$, (π, π^*) , $(\pi, 3p\sigma)$, and $(\pi, 3p\sigma')$. The symmetry and spectroscopic denotation for these five lowest-lying excited singlet states are $\tilde{A}(1^1A'')$, $\tilde{B}(2^1A'')$, $\tilde{C}(2^1A')$, $\tilde{D}(3^1A'')$, and $\tilde{E}(4^1A'')$, respectively. Some triplet states were also calculated. The triplets are found to lie below the first excited singlet state of $(\pi, 3s/\sigma_{C-Cl}^*)$ and could be responsible for the absorption spectrum of VC in the energy region of ~ 6 eV. It is noteworthy that the (π, π^*) state lies too high to be involved in the photodissociation of VC upon the excitation at 193 nm, in contradictory to the existing literature reports. Based on our calculations, the absorption spectrum of VC is analyzed comprehensively in 45 000–62 500 cm^{-1} for the first time, and will be discussed in the rest of this paper.

This paper is organized as follows. Section II describes the *ab initio* calculation methods. Section III depicts the calculated results and compares the simulated vibronic spectra of VC with the experiment. Photodissociation dynamics of VC at 193 nm is also discussed in this section. Finally, conclusions are addressed in Sec. IV.

II. METHOD

While the equilibrium geometries and normal-mode frequencies for both neutral and cationic VC in their ground states were computed using a MP2 method, the vibrational frequencies in the excited electronic states of neutral VC were calculated with a CIS method. The geometries of the five lowest-lying excited singlet states were optimized using a state-averaged CASSCF approach, in which the active space of (4, 13) was adopted. Accordingly, two valence orbitals of σ_{C-Cl}^* and π^* , in conjunction with the nine Rydberg orbitals of $3s$, $3p$, and $3d$, are all implemented in the calculation. The two occupied orbitals in the active space correspond to the π orbital of the C=C bond and a nonbonding one in the Cl atom which contains three lone pairs of electrons. Both vertical and adiabatic excitation energies were obtained with the state-averaged CASSCF, and refined by an internally contracted MRCI method including all single and double excitations from the occupied valence orbitals. The vertical excitation energies were calculated with the optimized ground-state geometry. To minimize systematic errors in calculating the states of different A' and A'' symmetries, we have lifted the Cl atom from the molecular plane by 0.1° , so that all calculations were performed in a C_1 group. Six states, including the ground and five excited singlet states, were averaged in the CASSCF calculations to render accurate excitation energies. In the MP2 and CIS calculations, a standard 6-311++G** basis set was utilized. In contrast, an extra diffuse *sp* function with a low exponent of 0.013 1928,⁴² which is critical in calculating Rydberg states, was added to the wave function of the C atom in the CASSCF and MRCI calculations. The MP2 and CIS calculations were performed using the GAUSSIAN 94 package,⁴³ whereas the CASSCF and MRCI calculations were carried out employing the MOLPRO 96 program.⁴⁴

The FCFs of VC have been calculated with the method developed by Mebel, Chen, and Lin.^{45,46} In the FCF calculations, we have made the following assumptions. First, the

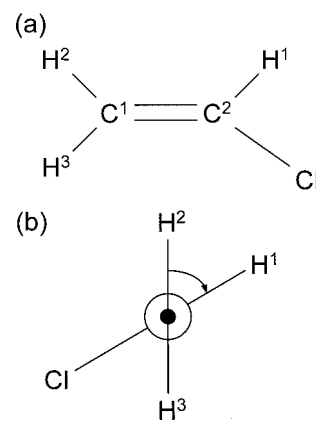


FIG. 1. Definition of geometry parameters used in the *ab initio* calculations of vinyl chloride.

potential energy surfaces in both ground and excited states are harmonic oscillators. Second, the two surfaces are displaced but not distorted. Finally, Duschinsky effects⁴⁷ (mode mixing) are neglected in the calculations. Accordingly, the square of the vibrational overlap integral, $|I_{a0bv}|^2$, for a transition from the zero-point vibration of ground state a to the v th quantum of a specific vibrational mode in the excited electronic state b is given by

$$|I_{a0bv}|^2 = \frac{S^v e^{-S}}{v!} \quad (1)$$

and

$$S = \frac{\omega(\Delta Q)^2}{2\hbar}, \quad (2)$$

where S is a Huang–Rhys factor, ΔQ is the displacement in terms of normal coordinates, ω is the vibrational frequency of the corresponding normal mode, and $h = 2\pi\hbar$ is the Planck constant.

III. RESULTS AND DISCUSSION

A. Optimized geometries and vibrational frequencies

Figure 1 shows the definition of geometrical parameters used in optimizing the structure of VC. Table I gives the calculated results for the ground and five lowest-lying excited states. The parameters CC, CCH, and HCCH stand for bond length (\AA), bending angle, and dihedral angle [Fig. 1(b)], respectively. The calculated geometry of the ground state is in agreement with experiment (Table I). For the excited states of VC, the promotion of a valence electron to an unoccupied orbital generally results in elongating the CC bond, shortening the CCl bond, and opening the HCCH angle (Table I). For example, the changes in the CC bond, CCl bond, and the HCCH angle of the $\tilde{D}(3^1A'')$ state with respect to the ground state are $+0.0862$ \AA , -0.0864 \AA , and $+3.8^\circ$, respectively. The $\tilde{E}(4^1A'')$ state, however, shows a little exception where the CCl bond is slightly longer than that of the ground state (Table I).

Although all calculations were performed without symmetry constraint (i.e., in a C_1 point group), most of the excited states are found planar, except $\tilde{C}(2^1A')$, i.e., the

TABLE I. Optimized geometries of vinyl chloride in the ground and five lowest-lying excited singlet states.^a

Parameter ^b	Expt. ^c	$\tilde{X}(1^1A')$	$\tilde{A}(1^1A'')$	$\tilde{B}(2^1A'')$	$\tilde{C}(2^1A')$	$\tilde{D}(3^1A'')$	$\tilde{E}(4^1A'')$
C ¹ C ²	1.332	1.3352	1.4004	1.4704	1.4508	1.4214	1.3929
C ² H ¹	1.079	1.0837	1.0774	1.0710	1.0825	1.0758	1.0745
C ¹ H ²	1.078	1.0844	1.0793	1.0720	1.0755	1.0744	1.0869
C ¹ H ³	1.090	1.0840	1.0745	1.0718	1.0740	1.0750	1.0822
C ² Cl	1.726	1.7289	1.6834	1.6507	1.6482	1.6425	1.7548
C ¹ C ² H ¹	123.8°	123.4°	120.6°	122.8°	121.0°	120.3°	122.3°
C ² C ¹ H ²	119.5°	119.1°	118.1°	119.2°	119.1°	119.3°	121.3°
H ² C ¹ H ³	119.5°	118.9°	120.4°	121.0°	120.1°	120.2°	119.4°
H ¹ C ² Cl	113.9°	113.5°	116.7°	117.4°	117.5°	117.3°	114.5°
H ² C ¹ C ² H ¹	0°	0°	0°	0°	13.3°	0°	0°

^aThe ground state is calculated at the MP2/6-311++G** level, while the others are at the CASSCF/6-311++G** level; see the text.

^bThe denotations of CC, CCH, and HCCH stand for bond length (Å), bending angle, and dihedral angle, respectively. For all electronic states, the H³, C¹, C², and H² atoms always form the same plane; the same is true for the Cl, C², C¹, and H¹ atoms.

^cExperimental values taken from Ref. 20.

(π, π^*) state (Table I). Moreover, the H³, H², C¹, and C² atoms always form a plane, and the same is true for the Cl, H¹, C², and C¹ atoms (Table I), indicating that the σ bonds of the two C atoms are more likely sp^2 hybridized. The $\tilde{C}(2^1A')$ state, corresponding to the $\pi^* \leftarrow \pi$ excitation, is expected to have a distorted structure with the two terminal groups of HCH and HCCl twisted along the CC bond according to Walsh rules.⁴⁸ In the CIS calculation where only a single excited orbital is considered, the dihedral angle of H²C¹C²H¹ for the (π, π^*) excited state is 90°, similar to the (π, π^*) state of ethylene (CH₂CH₂).^{42,46} In the CASSCF calculation, however, the twisting angle is reduced to 13.3° (Table I), because the wave function of the twisted (π, π^*) state is mixed with those of other excited (planar) states. Note that the symmetry denotation of $\tilde{C}(2^1A')$ is valid only if the VC molecule belongs to a C_s group; more precisely, the (π, π^*) excited state should be $\tilde{C}(4^1A)$, if all electronic states of VC are represented under C_1 molecular symmetry.

The calculated normal-mode frequencies are listed in Table II. For VC with C_s molecular symmetry, there are nine A' and three A'' vibrational modes. The vibrational frequencies in the ground states, for the neutral and the cationic VC, were calculated using the MP2 method and scaled by a factor

of 0.975. On the other hand, the vibrational frequencies in the \tilde{A} , \tilde{B} , and \tilde{E} excited states were obtained using the CIS method and scaled by 0.905. For the \tilde{C} state, the CIS calculation predicts a 90°-twisted geometry, as mentioned above, which is quite different from that optimized by the CASSCF method; the frequencies of the \tilde{C} state calculated by the CIS method are therefore not included in Table II. Meanwhile, we failed to optimize the $\tilde{D}(3^1A'')$ state using the CIS method, because calculations starting with different initial geometries of this state have finally converged to either $\tilde{A}(1^1A'')$ or $\tilde{B}(2^1A'')$ due to the mixing of wave functions. In principle, the vibrational frequencies of the \tilde{C} and \tilde{D} states can be computed by a more sophisticated CASSCF method. In the present study, however, we adopt the vibrational frequencies of the neutral and cationic VC to estimate those of the valence $\tilde{C}(2^1A')$ state and the Rydberg $\tilde{D}(3^1A'')$, respectively.

It can be seen from Table II that the distortion of potential energy surfaces can be neglected in the FCF calculations, especially for the A' vibrational modes, since the vibrational frequencies do not change drastically from the ground state to the excited states. The contribution to the FCFs resulting

TABLE II. Vibrational frequencies of vinyl chloride.^a

Symmetry	Mode	Vibration	Expt. ^b	$\tilde{X}(1^1A')$	$\tilde{A}(1^1A'')$	$\tilde{B}(2^1A'')$	$\tilde{E}(4^1A'')$	Cation
A'	ν_1	CH ₂ <i>a</i> . stretch	3121	3218	3105	3101	3110	3232
	ν_2	CH stretch	3086	3167	3007	2865	3094	3147
	ν_3	CH ₂ <i>s</i> . stretch	3030	3114	2932	2778	2945	3106
	ν_4	C=C stretch	1608	1613	1470	1458	1511	1500
	ν_5	CH ₂ bend	1370	1385	1364	1353	1340	1396
	ν_6	CH rock	1281	1293	1245	1171	1241	1270
	ν_7	CH ₂ rock	1031	1029	1036	1035	1011	1098
	ν_8	C-Cl stretch	721	735	773	760	810	869
	ν_9	C-Cl deform	395	394	365	374	378	399
A''	ν_{10}	CH ₂ wag	942	956	1016	1061	1135	965
	ν_{11}	CH wag	897	803	773	903	881	860
	ν_{12}	twist	620	599	356	418	439	388

^aThe ground state and the cation are calculated at the MP2/6-311++G** level and are scaled by 0.975, while the others are at the CIS/6-311++G** level and scaled by 0.905.

^bExperimental values are taken from Refs. 17–27.

TABLE III. Excitation energies (eV) and oscillator strengths of vinyl chloride for the transitions from the ground state to the five excited states.

Excited state	Character	Adiabatic energy		Vertical energy			Oscillator strength ^c
		CASSCF	MRCI	CASSCF	MRCI	CIS ^a	
$\tilde{A}(1^1A'')$	$(\pi, 3s/\sigma^*)$	6.41	6.66	6.52	6.68	7.13	5.15×10^{-2}
$\tilde{B}(2^1A'')$	$(\pi, \sigma^*/3s)$	6.62	6.74	7.10	7.27	7.62	3.70×10^{-3}
$\tilde{C}(2^1A')$	(π, π^*)	6.65	6.82	7.30	7.46	7.39 ^b	8.18×10^{-2}
$\tilde{D}(3^1A'')$	$(\pi, 3p\sigma)$	6.79	6.99	7.32	7.48	7.82	2.28×10^{-4}
$\tilde{E}(4^1A'')$	$(\pi, 3p\sigma')$	7.34	7.49	7.50	7.56	8.12	7.30×10^{-5}

^aExcitation energies calculated by the CIS method for the transitions from the ground state to the five lowest-lying excited triplet states are $\tilde{a}(1^3A')$ 3.45, $\tilde{b}(1^3A'')$ 6.91, $\tilde{c}(2^3A'')$ 6.99, $\tilde{d}(3^3A'')$ 7.71, and $\tilde{e}(4^3A'')$ 8.00 eV.

^bThe (π, π^*) state is the second excited state calculated by the CIS method, but is the third one with the higher-level CASSCF and MRCI calculations.

^cCalculated at the CASSCF/6-311++G** level.

from the distortion effect is less than 10%, estimated from assuming that the normal modes of the \tilde{A} , \tilde{B} , and \tilde{E} states are completely distorted but not displaced with respect to the ground state.⁴⁷ The estimated error is also supported by the calculated FCFs for the $(\pi, 3p\pi)$ Rydberg state of VC, which agrees with the experimental observation within an uncertainty limit of 10%.³⁰

B. Excitation energies and oscillator strengths

Table III presents the adiabatic and vertical excitation energies, together with oscillator strengths, for the transitions from the ground state to the five lowest-lying excited singlet states of VC. The five lowest-lying excited states are calculated to be ~ 6.4 – 7.5 eV above the ground state. The excitation energies were not corrected to the zero-point energies because the vibrational frequencies of the $\tilde{C}(2^1A')$ and $\tilde{D}(3^1A'')$ states were not calculated directly, as mentioned above. However, from the vibrational frequencies listed in Table II we can estimate the zero-point energy corrections to be less than 400 cm^{-1} (0.05 eV), which is within the calculation uncertainties (see Sec. III D).

Due to the mixing of wave functions, the first two excited states (Table III) can be attributed to either the $(\pi, \sigma_{\text{C-Cl}}^*)$ valence state or the $(\pi, 3s)$ Rydberg state. However, the $\tilde{A}(1^1A'')$ state has more $(\pi, 3s)$ character, while the $\tilde{B}(2^1A'')$ state is primarily contributed from the $(\pi, \sigma_{\text{C-Cl}}^*)$.

Accordingly, we denote the \tilde{A} and \tilde{B} states as $(\pi, 3s/\sigma_{\text{C-Cl}}^*)$ and $(\pi, \sigma_{\text{C-Cl}}^*/3s)$, respectively. On the other hand, the \tilde{C} state, resulting from the promotion of a π electron to the π^* orbital, has its adiabatic excitation energy of 6.65 eV and 6.82 eV, respectively, in the CASSCF and MRCI calculations. Finally, both \tilde{D} and \tilde{E} excited states are of $3p\sigma$ Rydberg character (Table III). Herein, we denote the in-plane (A' symmetry) and out-of-plane (A'' symmetry) $3p$ Rydberg orbitals as $3p\sigma$ and $3p\pi$, respectively. For VC, there are two $(\pi, 3p\sigma)$ and one $(\pi, 3p\pi)$.³⁰ The $(\pi, 3p\pi)$ Rydberg state of VC with an excitation energy of $63\,043 \text{ cm}^{-1}$ (7.82 eV) has been observed and analyzed in our previous 2+1 REMPI study.³⁰

Although the five lowest-lying excited singlet states of VC are all in the 6.4–7.5 eV region, only the transitions of $\tilde{A}(1^1A'') \leftarrow \tilde{X}(1^1A')$ and $\tilde{C}(2^1A') \leftarrow \tilde{X}(1^1A')$ have significant oscillator strengths of 5.15×10^{-2} and 8.18×10^{-2} , respectively (Table III). In other words, the $\tilde{A} \leftarrow \tilde{X}$ and $\tilde{C} \leftarrow \tilde{X}$ transitions dominate the observed one-photon absorption spectrum of VC within this energy range (see Sec. III D).

C. Franck–Condon factors

Table IV lists the displacements (ΔQ) and Huang–Rhys factors (S) of VC from which the Franck–Condon factors are

TABLE IV. Displacements (ΔQ) and Huang–Rhys factors (S) of vinyl chloride in the five lowest-lying excited singlet states with respect to the ground state.

Mode	ΔQ					S				
	$\tilde{A}(1^1A'')$	$\tilde{B}(2^1A'')$	$\tilde{C}(2^1A')$	$\tilde{D}(3^1A'')$	$\tilde{E}(4^1A'')$	$\tilde{A}(1^1A'')$	$\tilde{B}(2^1A'')$	$\tilde{C}(2^1A')$	$\tilde{D}(3^1A'')$	$\tilde{E}(4^1A'')$
ν_1	-0.0725	-0.1800	0.0154	-0.1224	-0.0040	0.2513	1.5473	0.0113	0.7173	0.0008
ν_2	0.0116	0.0077	0.0127	0.0187	0.0020	0.0064	0.0028	0.0076	0.0164	0.0002
ν_3	0.0177	0.0209	-0.0294	0.0181	0.0277	0.0145	0.0203	0.0400	0.0151	0.0355
ν_4	0.0814	0.1385	0.1129	0.1002	0.0513	0.1586	0.4590	0.3051	0.2319	0.0629
ν_5	-0.0719	-0.1464	0.0511	-0.0998	-0.0753	0.1062	0.4406	0.0537	0.2057	0.1166
ν_6	0.0600	0.0995	-0.0875	0.0818	-0.0248	0.0691	0.1900	0.1470	0.1271	0.0118
ν_7	0.0336	0.1538	-0.0184	0.0946	0.0484	0.0172	0.3613	0.0052	0.1413	0.0358
ν_8	0.0509	0.2102	-0.0851	0.0716	0.1504	0.0283	0.4822	0.0790	0.0611	0.2470
ν_9	-0.1025	-0.3763	0.0010	-0.2180	-0.0004	0.0614	0.8281	0	0.2797	0
ν_{10}	0	0	-0.1892	0	0	0	0	0.5067	0	0
ν_{11}	0	0	-0.0907	0	0	0	0	0.0980	0	0
ν_{12}	0	0	-0.2125	0	0	0	0	0.4005	0	0

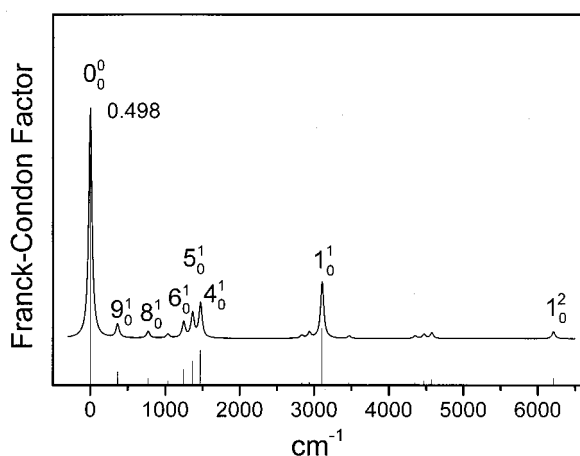


FIG. 2. Franck–Condon factors (sticks) and predicted vibronic spectrum for the $\tilde{A}(1^1A'') \leftarrow \tilde{X}(1^1A')$ transitions.

calculated. Figures 2–6 depict the Franck–Condon factors (stick diagrams) and simulated absorption spectra (lines) of VC for the transitions from the ground state to the five lowest-lying excited singlet states. In the simulated spectra, a Lorentzian line shape with an arbitrary full width at half maximum (FWHM) of 50 cm^{-1} has been implemented to each peak. The Lorentzian shape functions are chosen based on our previous REMPI spectroscopic study on the $3p\pi \leftarrow \pi$ transition of VC.³⁰

For simplicity, only the Franck–Condon factors of the origin bands are given explicitly in Figs. 2–6; the stronger vibronic bands are also marked in the figures. For the $\tilde{A} \leftarrow \tilde{X}$ transition, the active modes (with large FCFs) are ν_1 , ν_{4-6} , and $\nu_{8,9}$ (Fig. 2). The $\tilde{B} \leftarrow \tilde{X}$ transition is characterized by a long vibrational progression of the ν_1 mode (Fig. 3). Due to a twisted geometry in the \tilde{C} state, the ν_{10} , ν_{11} , and ν_{12} modes (of A'' symmetry in a C_s group, but of A symmetry if under a C_1 group) are also activated in the $\tilde{C} \leftarrow \tilde{X}$ transition (Fig. 4); otherwise for other planar excited states, only the vibrational modes of A' symmetry are visible. It is noted that similar active vibrational modes are found in the

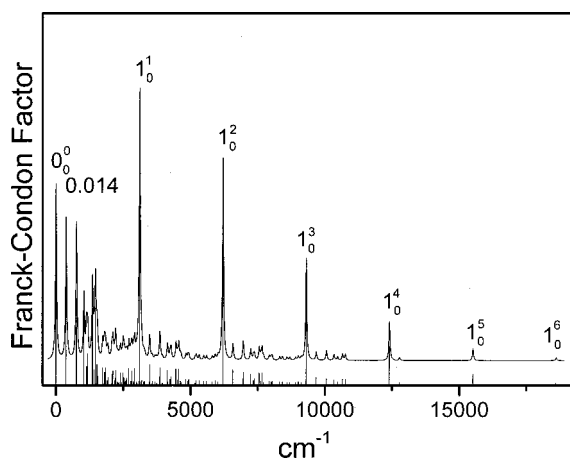


FIG. 3. Franck–Condon factors (sticks) and predicted vibronic spectrum for the $\tilde{B}(2^1A'') \leftarrow \tilde{X}(1^1A')$ transitions.

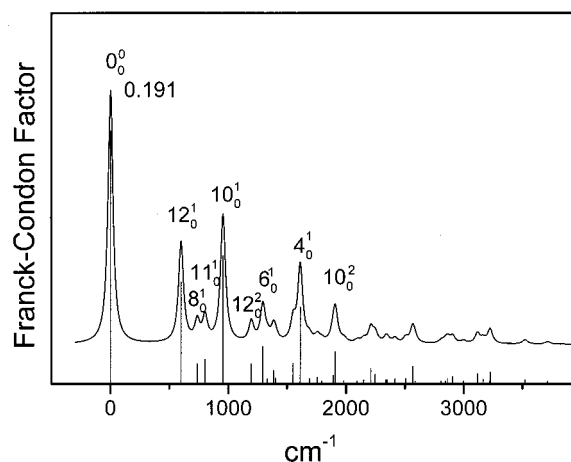


FIG. 4. Franck–Condon factors (sticks) and predicted vibronic spectrum for the $\tilde{C}(2^1A') \leftarrow \tilde{X}(1^1A')$ transitions.

$\tilde{A} \leftarrow \tilde{X}$, $\tilde{B} \leftarrow \tilde{X}$, and $\tilde{D} \leftarrow \tilde{X}$ transitions (Figs. 2, 3, and 5). As can be seen in Fig. 6, the ν_{3-5} , ν_7 , and ν_8 vibrational modes dominate the spectral pattern of the $\tilde{E} \leftarrow \tilde{X}$ transition. In general, overtones and combination bands appear as weaker peaks in the vibronic spectra of VC (Figs. 2 and 4–6).

D. Absorption spectra

In this section, we compare our calculations with the experimental results. The vibronic transition probability includes the electronic oscillator strength and the calculated vibrational FCF. Each vibronic band was convoluted with Lorentzian line shape to render theoretical absorption spectra. Various widths of the line functions have been tested to simulate the observed spectrum. Figure 7 compares the simulated vibronic spectrum of VC [Fig. 7(b) with a FWHM = 500 cm^{-1} for each vibronic transition] with that recorded by Berry [Fig. 7(a)].¹⁴ The adiabatic excitation energies calculated by the internally contracted MRCI method (Table III) have been used to locate the theoretical spectrum in Fig. 7(b). Although all transitions from the ground state to the five lowest-lying excited singlet states have been included

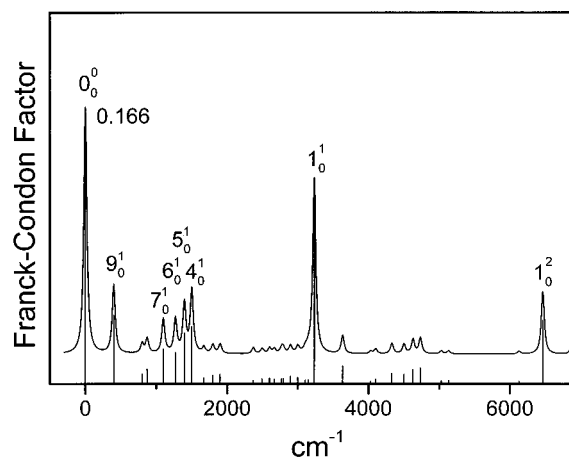


FIG. 5. Franck–Condon factors (sticks) and predicted vibronic spectrum for the $\tilde{D}(3^1A'') \leftarrow \tilde{X}(1^1A')$ transitions.

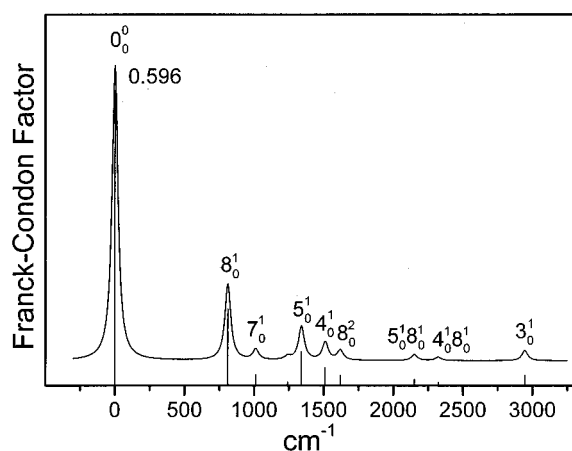


FIG. 6. Franck-Condon factors (sticks) and predicted vibronic spectrum for the $\tilde{E}(4^1A') \leftarrow \tilde{X}(1^1A')$ transitions.

for the simulated spectrum, the prominent peaks in Fig. 7(b) are mainly contributed from the $\tilde{A} \leftarrow \tilde{X}$ and $\tilde{C} \leftarrow \tilde{X}$ transitions because of their larger oscillator strengths (Table III). The simulated spectrum [Fig. 7(b)] is in satisfactory agreement with experiment [Fig. 7(a)] based on the following examinations. First, both spectra show a broad and continuous feature at 52 500–60 000 cm^{-1} . Second, the strongest peak at 53 720 cm^{-1} in the calculation, corresponding to the origin band of the $3s/\sigma_{\text{C-Cl}}^* \leftarrow \pi$ transition, is close to the maximum spectral intensity observed at $\sim 54\,140$ cm^{-1} . Taking the AIE of 80 720 cm^{-1} for VC as we determined in the previous studies,^{29,30} the assignment of the 54 140 cm^{-1} peak as due to $(\pi, 3s)$ renders a quantum defect of 0.97, which in return justifies the assignment for an s Rydberg state of a hydrocarbon molecule. Identifying this peak also supports our previous assignments for the (π, n, s) Rydberg series,³⁰ because the other labeling as due to a $(\pi, (n-1)d)$ Rydberg series by Williams and Cool³⁷ would attribute this Rydberg member to

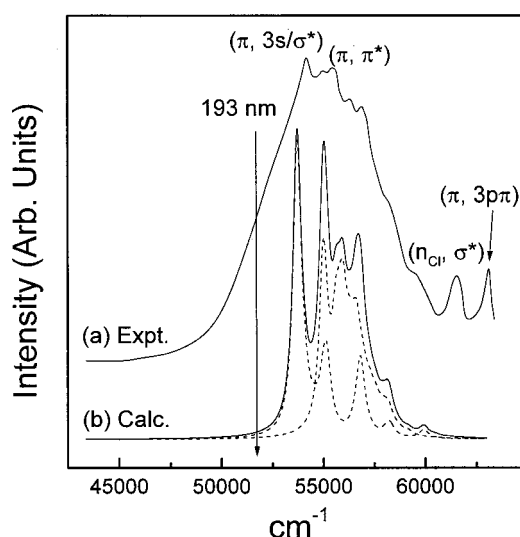


FIG. 7. (a) Experimental absorption spectrum (upper) of vinyl chloride taken from Ref. 14 and (b) simulated vibronic spectrum (lower). The dashed lines represent the spectra resulting from the $3s/\sigma^* \leftarrow \pi$ and $\pi^* \leftarrow \pi$ transitions.

a nonexistent $(\pi, 2d)$ state. Third, the next strong peak predicted by the calculation is the $\pi^* \leftarrow \pi$ transition around 55 000 cm^{-1} , where the experimental spectra show similar behaviors (Fig. 7). We propose that the two observed peaks at 55 030 and 55 530 cm^{-1} are possible candidates for the $\pi^* \leftarrow \pi$ transition. The origin band of the $\pi^* \leftarrow \pi$ transition is less intense than that of $3s/\sigma_{\text{C-Cl}}^* \leftarrow \pi$ [Fig. 7(b), dashed lines] owing to a larger FCF for the latter (Figs. 2 and 3), although the former has larger oscillator strength (Table III). If our assignments for the $(\pi, 3s/\sigma_{\text{C-Cl}}^*)$ and (π, π^*) states are correct, a small error of 0.07 eV is resulted from the comparison between calculation and experiment. However, we recognize that an uncertainty of 0.2 eV is generally estimated for the MRCI calculations according to previous experiences.^{45–47} Finally, the intensities in both theoretical and experimental spectra decline gradually from 55 000 to 60 000 cm^{-1} , accompanied with several weak peaks on the shoulder. In the present study, the shoulder peaks cannot be assigned without ambiguity, because of the overlapping of congested vibronic transitions.

Above 60 000 cm^{-1} , a peak is observed at 61 650 cm^{-1} (with FWHM ~ 700 cm^{-1}) which is quite separate from other congested bands [Fig. 7(a)] and should correspond to the signal we observed at 61 500 cm^{-1} using REMPI spectroscopy.³⁰ We assign this peak as the $\sigma_{\text{C-Cl}}^* \leftarrow n_{\text{Cl}}$ transition of VC based on the CIS calculation (not shown), which indicates that the energy of the $(n_{\text{Cl}}, \sigma_{\text{C-Cl}}^*)$ excited state is slightly higher than the five lowest-lying excited states. In general, the promotion of a nonbonding electron into an excited orbital causes little geometrical change, and therefore only the origin band is active in the absorption spectra according to the Franck-Condon principle.⁴⁹ This is in agreement with the observed peak at 61 650 cm^{-1} without long vibrational progressions.

The absorption spectrum of VC shows a long tail in the lower frequency side around 45 000–54 000 cm^{-1} [Fig. 7(a)], which however cannot be attributed to the transitions excited from the ground state to the five lowest-lying excited singlet states [Fig. 7(b)]. Hot-band transitions could contribute some intensity near the first (strongest) peak at 54 140 cm^{-1} [Fig. 7(a)]. According to the following calculation, this tail could be due to the transitions from the ground state of VC to excited triplet states. The vertical excitation energies for five triplet-singlet transitions have been calculated at the CIS/6-311++G** level (Table III). Three excited triplet states [i.e., $\tilde{a}(1^3A')$, $\tilde{b}(1^3A'')$ and $\tilde{c}(2^3A'')$] are found to lie below the first excited singlet state $\tilde{A}(1^1A')$. The first excited triplet state of VC has been observed at 3.4–5.1 eV by Koerting *et al.*¹⁶ using low energy electron-impact energy-loss spectroscopy, in agreement with our calculation [3.45 eV for $\tilde{a}(1^3A')$ in Table III]. The calculated energies for the $\tilde{b}(1^3A'')$ and $\tilde{c}(2^3A'')$ states falls within the energy region of 45 000–54 000 cm^{-1} . The $\tilde{b}(1^3A'') \leftarrow \tilde{X}(1^1A')$ and $\tilde{c}(2^3A'') \leftarrow \tilde{X}(1^1A')$ transitions could be involved in the absorption spectrum of VC at 45 000–54 000 cm^{-1} [Fig. 7(a)]. The appearance of these spin-forbidden transitions in the spectrum could be due to an intensity borrowing from the

nearby (same symmetry) $\tilde{A}(1^1A'')$ excited state, through spin-orbit coupling caused by the Cl atom.

In previous theoretical study of VC, Umemoto *et al.*¹¹ calculated the relative energies of the (π, σ_{C-Cl}^*) , (π, π^*) , (n_{Cl}, π^*) , and $(n_{Cl}, \sigma_{C-Cl}^*)$ excited states using *ab initio* methods with double-zeta quality 4-31G basis sets. The (π, σ_{C-Cl}^*) state is regarded as the first excited state of VC in their calculation but without definite excitation energy. Using the MRCI method with cc-pVTZ basis set, Tonokura *et al.*⁷ calculated the vertical excitation energies of 7.262, 7.399, 7.897, and 8.490 eV for the $\sigma_{C-Cl}^* \leftarrow \pi$, $\pi^* \leftarrow \pi$, $\pi^* \leftarrow n_{Cl}$, and $\sigma_{C-Cl}^* \leftarrow n_{Cl}$ transitions of VC, respectively. Browning *et al.*³⁸ calculated the vertical excitation energy for the $\pi^* \leftarrow \pi$ transition of VC to be 7.8227 eV at the CIS/6-311G* level. Compared with experiment, however, none of these calculated results can nicely account for the absorption spectrum of VC [Fig. 7(a)]. For instance, the first excited singlet state predicted by Tonokura *et al.*⁷ would appear in the vicinity of 58 570 cm^{-1} , but the actual absorption intensity of VC increases from $\sim 45\,000\ \text{cm}^{-1}$ and reaches a maximum at 54 140 cm^{-1} [Fig. 7(a)].¹⁴ On the other hand, our calculations match quite satisfactorily with the observed absorption spectrum of VC at 52 500–60 000 cm^{-1} . The different results obtained in our calculation and that of Tonokura *et al.*⁷ stem from different choices of the active space for the excited electrons employed in the computations. In this study, we have used a (4, 13) active space, i.e., four electrons are allowed to distribute among two occupied, two valence, and nine Rydberg orbitals, while in the calculation by Tonokura *et al.*⁷ a (8, 6) active space was adopted where only two valence orbitals are considered but with much emphasis on the four occupied ones. Without taking Rydberg orbitals into account, we believe that Tonokura *et al.*⁷ overlooked the contribution from the (low-lying) Rydberg states in their calculation.

Photodissociation of VC excited at the convenient wavelength of 193 nm with an ArF laser has been heavily explored in the past decades.^{1–11} It was generally conceived that the (π, π^*) state of VC was excited in the photoabsorption at 193 nm (51 800 cm^{-1}).⁶ In the wake of the $\pi^* \leftarrow \pi$ excitation, various dissociation channels were taken to the (π, σ_{C-Cl}^*) excited-state or the ground-state potential energy surface, probably via internal conversions.⁶ This kind of arguments was usually concluded from measuring the velocity and angular distributions of photofragments, but the correlated excited states involved in the photodissociation pathways were rarely verified theoretically. The highest-level theoretical examination of VC before this study was that of Tonokura *et al.*⁷ Based on the present calculation, the $(\pi, 3s/\sigma_{C-Cl}^*)$ and (π, π^*) states are too high to be reached with the 193 nm excitation (Fig. 7), and we believe that the $\tilde{b}(1^3A'')$ and $\tilde{c}(2^3A'')$ excited state could be responsible for the excitation of VC at 193 nm.

IV. CONCLUSION

We have performed *ab initio* calculations of equilibrium geometries, excitation energies, oscillator strengths, and Franck-Condon factors to investigate the low-lying elec-

tronic states of VC. The five lowest-lying excited singlet states of VC, i.e., $(\pi, 3s/\sigma_{C-Cl}^*)$, $(\pi, \sigma_{C-Cl}^*/3s)$, (π, π^*) , $(\pi, 3p\sigma)$, and $(\pi, 3p\sigma')$, are found to be clustered together at 6.4–7.5 eV. Among these five excited states, only the $3s/\sigma_{C-Cl}^* \leftarrow \pi$ and $\pi^* \leftarrow \pi$ transitions have significant oscillator strengths to appear in the observed absorption spectrum. The simulated absorption spectrum of VC is in satisfactory agreement with the observation.

In the one-photon absorption spectrum of VC, a long tail was observed at 45 000–54 000 cm^{-1} and was speculated due to the $\tilde{b}(1^3A'') \leftarrow \tilde{X}(1^1A')$ and $\tilde{c}(2^3A'') \leftarrow \tilde{X}(1^1A')$ transitions via the spin-orbit coupling caused by the Cl atom. This is in contrast to the existing literature reports that the (π, π^*) state of VC was excited in the absorption of 193 nm photons. Theoretical investigations on the triplet excited states of VC using high-level *ab initio* calculation methods are under way. Re-examination of the photodissociation of VC at 193 nm is also suggested taking these triplet states into account.

ACKNOWLEDGMENTS

The authors thank Hsiu-Ling Lin and Dr. A. M. Mebel for their assistance in the early *ab initio* calculations for the excited vinyl chloride. J.L.C. is grateful to Academia Sinica fellowship during his postdoctoral career at IAMS, and expresses his appreciation of the encouragement from Director S. H. Lin over the course of this work. This research is supported by the National Science Council of ROC (Grant No. NSC-90-2113-M-001-037) and China Petroleum Corporation.

- ¹P. T. A. Reilly, Y. Xie, and R. J. Gordon, *Chem. Phys. Lett.* **178**, 511 (1991).
- ²Y. Mo, K. Tonokura, Y. Matsumi, M. Kawasaki, T. Sato, T. Arikawa, P. T. A. Reilly, Y. Xie, Y.-A. Yang, Y. Huang, and R. J. Gordon, *J. Chem. Phys.* **97**, 4815 (1992).
- ³Y. Huang, Y.-A. Yang, G. He, and R. J. Gordon, *J. Chem. Phys.* **99**, 2752 (1993).
- ⁴Y. Huang, Y.-A. Yang, G. He, and R. J. Gordon, *J. Chem. Phys.* **103**, 5476 (1995).
- ⁵G. He, Y. Yang, Y. Huang, S. Hashimoto, and R. J. Gordon, *J. Chem. Phys.* **103**, 5488 (1995).
- ⁶D. A. Blank, W. Sun, A. G. Suits, Y. T. Lee, S. W. North, and G. E. Hall, *J. Chem. Phys.* **108**, 5414 (1998).
- ⁷K. Tonokura, L. B. Daniels, T. Suzuki, and K. Yamashita, *J. Phys. Chem. A* **101**, 7754 (1997).
- ⁸D. J. Donaldson and S. R. Lenone, *Chem. Phys. Lett.* **132**, 240 (1986).
- ⁹M. G. Moss, M. D. Ensminger, and J. D. McDonald, *J. Chem. Phys.* **74**, 6631 (1981).
- ¹⁰S.-R. Lin, S.-C. Lin, Y.-C. Lee, Y.-C. Chou, I.-C. Chen, and Y.-P. Lee, *J. Chem. Phys.* **114**, 160 (2001).
- ¹¹M. Umemoto, K. Seki, H. Shinohara, U. Nagashima, N. Nishi, M. Kinoshita, and R. Shimada, *J. Chem. Phys.* **83**, 1657 (1985).
- ¹²A. D. Walsh, *Trans. Faraday Soc.* **41**, 35 (1945).
- ¹³S. P. Sood and K. Watanabe, *J. Chem. Phys.* **45**, 2913 (1966).
- ¹⁴M. J. Berry, *J. Chem. Phys.* **61**, 3114 (1974).
- ¹⁵R. Locht, B. Leyh, K. Hottmann, and H. Baumgärtel, *Chem. Phys.* **220**, 207 (1997).
- ¹⁶C. F. Koerting, K. N. Walzl, and A. Kuppermann, *Chem. Phys. Lett.* **109**, 140 (1984).
- ¹⁷C. W. Gullikson and J. R. Nielsen, *J. Mol. Spectrosc.* **1**, 158 (1957).
- ¹⁸S. Narita, S. Ichinohe, and S. Enomoto, *J. Chem. Phys.* **31**, 1151 (1959).
- ¹⁹D. Kivelson and E. B. Wilson, Jr., *J. Chem. Phys.* **32**, 205 (1960).
- ²⁰M. Hayashi and T. Inagusa, *J. Mol. Struct.* **220**, 103 (1990).

- ²¹S. Giorgianni, A. de Lorenzi, M. Pedrali, P. Stoppa, and S. Gherseti, *J. Mol. Spectrosc.* **156**, 373 (1992).
- ²²S. Giorgianni, A. de Lorenzi, P. Stoppa, A. Baldan, and S. Gherseti, *J. Mol. Spectrosc.* **164**, 550 (1994).
- ²³I. Merke, L. Poteau, G. Wlodarczak, A. Bouddou, and J. Demaison, *J. Mol. Spectrosc.* **177**, 232 (1996).
- ²⁴P. Stoppa, S. Giorgianni, and S. Gherseti, *Mol. Phys.* **91**, 215 (1997).
- ²⁵S. Giorgianni, P. Stoppa, and A. de Lorenzi, *Mol. Phys.* **92**, 301 (1997).
- ²⁶A. de Lorenzi, S. Giorgianni, and R. Bini, *Mol. Phys.* **96**, 101 (1999).
- ²⁷A. de Lorenzi, S. Giorgianni, and R. Bini, *Mol. Phys.* **98**, 355 (2000).
- ²⁸M. B. Robin, *Higher Excited States of Polyatomic Molecules* (Academic, New York, 1985), Vol. 3.
- ²⁹J.-L. Chang, J.-C. Shieh, J.-C. Wu, R. Li, and Y.-T. Chen, *Chem. Phys. Lett.* **325**, 369 (2000).
- ³⁰J.-L. Chang, R. Li, J.-C. Wu, J.-C. Shieh, and Y.-T. Chen, *J. Chem. Phys.* **115**, 5925 (2001).
- ³¹R. F. Lake and H. Thompson, *Proc. R. Soc. London, Ser. A* **315**, 323 (1970).
- ³²G. W. Mines and H. Thompson, *Spectrochim. Acta, Part A* **29**, 1377 (1973).
- ³³K. Wittel and H. Bock, *Chem. Ber.* **107**, 317 (1974).
- ³⁴K. H. Sze, C. E. Brion, A. Katrib, and B. El-Issa, *Chem. Phys.* **137**, 369 (1989).
- ³⁵L. Sheng, F. Qi, L. Tao, Y. Zhang, S. Yu, C.-K. Wong, and W.-K. Li, *Int. J. Mass Spectrom. Ion Processes* **148**, 179 (1995).
- ³⁶R. Locht, B. Leyh, K. Hottmann, and H. Baumgärtel, *Chem. Phys.* **220**, 217 (1997).
- ³⁷B. A. Williams and T. A. Cool, *J. Phys. Chem.* **97**, 1270 (1993).
- ³⁸P. W. Browning, D. C. Kitchen, M. F. Arendt, and L. J. Butler, *J. Phys. Chem.* **100**, 7765 (1996).
- ³⁹K. Takeshita, *Theor. Chem. Acc.* **101**, 343 (1999).
- ⁴⁰J. Riehl and K. Morokuma, *J. Chem. Phys.* **100**, 8976 (1994).
- ⁴¹B. T. Colegrove and T. B. Thompson, *J. Chem. Phys.* **106**, 1480 (1997).
- ⁴²K. B. Wiberg, C. M. Hadad, J. B. Foresman, and W. A. Chupka, *J. Phys. Chem.* **96**, 10756 (1992).
- ⁴³M. J. Frisch, G. W. Trucks, H. B. Schlegel, *et al.*, GAUSSIAN 94, Revision D. 4 Gaussian, Inc., Pittsburgh, PA, 1995.
- ⁴⁴MOLPRO 96 is a package of *ab initio* programs written by H.-J. Werner and P. J. Knowles, with contributions from J. Almlöf, R. D. Amos, M. J. O. Deegan, S. T. Elbert, C. Hampel, W. Meyer, K. Peterson, R. Pitzer, A. J. Stone, P. R. Taylor, and R. Lindh, University of Birmingham, Birmingham, UK, 1996.
- ⁴⁵A. M. Mebel, Y.-T. Chen, and S. H. Lin, *Chem. Phys. Lett.* **258**, 53 (1996).
- ⁴⁶A. M. Mebel, Y.-T. Chen, and S. H. Lin, *J. Chem. Phys.* **105**, 9007 (1996).
- ⁴⁷A. M. Mebel, M. Hayashi, K. K. Liang, and S. H. Lin, *J. Phys. Chem. A* **103**, 10674 (1999).
- ⁴⁸G. Herzberg, *Molecular Spectra and Molecular Structure. III* (Van Nostrand-Reinhold, New York, 1966).
- ⁴⁹P. F. Bernath, *Spectra of Atoms and Molecules* (Oxford, New York, 1995).